

## Article

# Experimental Study on the Influence of Humidity on Double-K Fracture Toughness and Fracture Energy of Concrete under Water Environment

Guohui Zhang \*, Xinlan Ni, Xiong Wei, Zhendong Yang and Yanshuang Gu

Electrical Engineering College, Kunming University of Science and Technology, Kunming 650500, China

\* Correspondence: zgh\_water@kust.edu.cn; Tel.: +86-1366-976-7383

**Abstract:** Saturated concrete is significantly different from dry concrete in fracture mechanical properties. Using the wedge-splitting tensile method to research the rule of change in moisture content, double-K fracture toughness and fracture energy of three strength grades (C20, C30, and C40) of concrete immersed in a free water environment for 0 h, 2 h, 5 h, 24 h, and 120 h were studied in order to provide support for the safety evaluation of concrete structures in a water environment. The initial cracking fracture toughness of C20, C30, and C40 concrete in saturated state were, respectively, 29.6%, 23.2%, and 33.4% lower than that in dry state. The unstable fracture toughness of C20, C30, and C40 concrete in saturated state were, respectively, 22.7%, 23.9% and 33.8% lower than that in dry state. The fracture energy of C20, C30, and C40 concrete in saturated state are only 71.99%, 70.29%, and 66.11% of that in dry state, respectively. The initial cracking fracture toughness and unstable fracture toughness of concrete all show a linear, decreasing trend with an increase in moisture content. Before the crack initiation, the measured  $P$ - $CMOD$  curve had an obvious linear elastic stage, stable expansion stage, and unstable expansion stage. The critical crack opening displacement gradually decreases with an increase in moisture content; the deformation capacity and toughness of concrete are shown to decrease. The humidity state should be fully considered when evaluating the fracture mechanical properties of concrete.

**Keywords:** hygrometric state concrete; moisture content; double-K fracture characteristics; cracking fracture toughness; fracture energy; wedge-splitting test



**Citation:** Zhang, G.; Ni, X.; Wei, X.; Yang, Z.; Gu, Y. Experimental Study on the Influence of Humidity on Double-K Fracture Toughness and Fracture Energy of Concrete under Water Environment. *Buildings* **2023**, *13*, 816. <https://doi.org/10.3390/buildings13030816>

Academic Editor: Ahmed Senouci

Received: 17 February 2023

Revised: 6 March 2023

Accepted: 12 March 2023

Published: 20 March 2023



**Copyright:** © 2023 by the authors. Licensee MDPI, Basel, Switzerland. This article is an open access article distributed under the terms and conditions of the Creative Commons Attribution (CC BY) license (<https://creativecommons.org/licenses/by/4.0/>).

## 1. Introduction

Concrete is one of the most important civil engineering materials. It is made of cementitious material, granular aggregate, and water according to a certain proportion of preparation. It is a kind of artificial stone which is formed by mixing, forming, and curing. Concrete is a multi-phase, composite material with initial microcracks and pores. As a typical quasi-brittle material, its fracture and damage mechanisms are extremely complex; the tensile strength of concrete is lower than the compressive strength and the crack resistance of concrete is weak [1,2]. Primary crack propagation is easily triggered by various complex factors, which leads to the damage and destruction of concrete structures. Concrete structures, such as dams and bridge piers used in water environments, often exist in different moisture content states [3–5]. The various deterioration in reinforced concrete structures is determined by moisture movement, which is the essential characteristic of concrete [6]. Existing studies have shown that there are significant differences in mechanical properties between wet concrete and normal concrete. For example, the ultimate compressive strength of concrete decreases with the increase of moisture content [7–10]. The dynamic tensile and compressive strength of wet concrete are influenced by the interaction between the loading rate and the moisture content [11]. Therefore, the mechanical indexes of normal concrete are more difficult to accurately evaluate than the mechanical properties of wet concrete. Noborn YUASA showed the inhomogeneous distribution of moisture content and porosity

from the surface layer to the internal parts of dried concrete. The inhomogeneity at the surface layer of structural concretes is also studied in terms of pore structures and moisture distributions associated with a drying immediately after the demolding [12].

At present, researchers pay more attention to the influence of moisture content on concrete strength, elastic modulus, and other indicators. Wang Hailong [13] prepared concrete specimens with different moisture content states by using the vacuum water saturation method, and experimental studies were conducted. The results showed that the compressive strength of concrete gradually decreases with an increase in moisture content. By conducting mechanical tests on four different concrete strength grades in seawater immersion, Han Yang found that the axial compressive strength of concrete shows a wavy decrease with the increase of soaking time, while the elastic modulus and Poisson's ratio gradually increase [14]. Huang [15] studied the influence of the first soaking age on the wet expansion of dam concrete, and the results showed that the wet expansion strain of concrete gradually increases with the increase of soaking time until it becomes stable. The influence of moisture content on the tensile adhesion performance of 3D-printable concrete was studied; an increased moisture content enhanced the tensile adhesion in the fresh state due to surface tension, while it reduced the tensile adhesion in the hardened state in the context of 3D concrete printing, which could be attributed to a higher water-to-cement ratio at the contact zone [16]. Pengju Zhang's results demonstrated that microwave power and moisture content are two important factors affecting the concrete's breaking [17]. The results showed that the freeze–thaw damage has a significant weakening effect on the fracture characteristics of concrete beams. The elastic modulus  $E$ , critical crack length  $a_c$ , fracture toughness  $K_{IC}$ , fracture energy  $G_F$ , and critical crack tip opening displacement  $CTOD_c$  of concrete beams all show a linear, decreasing trend with the increase of the number of  $F_T$  cycles [18]. Existing studies have shown that the mechanical properties of wet concrete are significantly different from normal concrete. For example, the ultimate compressive strength of concrete decreases with the increase of moisture content. Lu [19] researched the bonding properties of CFRP-concrete interface under the condition of humidity in three different epoxy resins. It was found that the ultimate strain, interfacial fracture energy, and ultimate load transferred to the CFRP plate tend to increase first and decrease or fluctuate second with time under the action of moisture. The results showed that both the mode I and mode II fracture energy release rates of CFRP-to-concrete interface decrease nonlinearly with salt moisture content, and the change of failure mode from debonding within the concrete layer to cohesive failure along the interface is also observed [20]. In terms of concrete fracture characteristics, researchers studied normal concrete fracture characteristics such as curing conditions, different height ratio, hydraulic pressure, freeze–thaw cycle, and others [21–24]. Testing methods for the determination of unstable cracking or failure for predicting crack the double-K criterion for crack propagation in concrete using wedge-splitting tests and three-point bending beam tests were invented by Reinhardt and Xu [25–27]. Gao Xiaofeng [28] studied the size effect on the fracture performance of wet-screened concrete using the wedge-splitting method and double-K fracture criterion. When the effective height of the specimen reached 500 mm, the results were obtained for stable fracture toughness, unstable fracture toughness, and fracture energy. Xu [29] carried out and discussed the cyclic test results of the double-K criterion for concrete crack growth, and it was observed that the double-K fracture parameters are almost independent to the type of initial notch.

Concurrently, some researchers have also carried out research on the fracture mechanical characteristics of wet concrete. Liu Hengjie [30] indirectly characterized the variation rule of concrete fracture mechanical properties under different moisture contents by comparing different emission signals. It was found that AE parameter values and cumulative values in the fracture process show a decreasing trend with the increase of moisture content. Zhang Guohui [31,32] carried out a three-point bending beam test. It was found that the fracture toughness of concrete decreases with the increase of moisture content, and that the fracture toughness of C15 concrete in the saturated state is decreased by 57%, compared

with that in dry state. An evaluation of fracture behavior of high-strength hydraulic concrete damaged by freeze-thaw cycle test and the assessment of interfacial fracture energy between concrete and CFRP under water immersion conditions were studied, and the interfacial fracture energy considerably dropped first and then leveled off during the first six months of immersion in water [33]. The fracture mechanical properties of concrete under 0–4 MPa hydraulic pressure were studied by researchers, and the results showed that high-pressure water damage significantly influences the concrete fracture performance, resulting in a faster failure process, poorer bearing capacity, and higher cracking susceptibility [34].

In essence, the current research on the physical and mechanical properties of wet concrete mainly focuses on the strength and deformation properties. Meanwhile, some scholars have also begun to pay attention to the evolution rule of fracture mechanical properties about the physical and mechanical properties of wet concrete. The research scope of moisture content mainly focuses on the dry or saturated limit humidity state, and the lack of an intermediate moisture content state makes the research on the influence rule of humidity on the fracture mechanical properties of concrete not systematic. Most studies use a three-point bending beam test to study the fracture mechanical properties of concrete. However, the influence of a three-point bending beam specimen caused by its self-weight cannot be eliminated well. Moreover, the three-point bending beam specimen has the disadvantages of considerable size in the length direction and a low material utilization rate. The wedge-splitting method can better offset the dead weight and vertical force, and the operation is straightforward [35]. Therefore, it is necessary to study the fracture mechanical properties of concrete with different moisture content based on wedge-splitting systems. The variation rule of concrete fracture characteristic parameters is based on the double-K fracture theory under other moisture content conditions. Additionally, the influence of moisture content on substantial fracture performance is systematically studied, which provides the basis for disaster evolution and safety evaluation of concrete structures under a water environment.

## 2. Experimental Program

### 2.1. Experimental Materials and Equipment

The cement was P•C 42.5 composite Portland cement, the water consumption of standard consistency was 26.2%, the stability was qualified, the initial setting time was 4.3 h, and the final setting time was 5.4 h. The fine aggregate was made of machined sand with a fineness modulus of 3.1, mud content of 0.2%, apparent density of 2750 kg/m<sup>3</sup>, and a bulk density of 1610 kg/m<sup>3</sup>. The content of harmful substances was below the specified value. The coarse aggregate was composed of 5–20 mm and 20–40 mm gravel with 0.5% mud content, 2750 kg/m<sup>3</sup> apparent density, and 1480 kg/m<sup>3</sup> bulk density. Tap water was used for the test. The concrete slump was 30–50 mm. The water–cement ratio of concrete was 0.7 with high value; thus, the concrete was not used for low-permeability hydraulic concretes. The concrete mix ratio was calculated by «Code For Design Of Hydraulic Concrete Mix» (DL/T5330—2015) [36]. The grades of concrete strength in this paper were set as C20, C30, and C40. The concrete mix ratio per cubic meter is shown in Table 1.

**Table 1.** Concrete mix ratio and main parameters.

Strength Grade	Sand Ratio (%)	Water Cement Ratio	Mix Ratio (kg/m <sup>3</sup> )				
			Water	Cement	Sand	Small Stone	Medium Stone
C20	44	0.70	165	236	906	577	577
C30	42	0.57	165	290	842	582	582
C40	41	0.55	162	295	821	591	591

The experiment adopted the universal servo testing machine in the TY-8000 series, produced by Jiangsu Tianyuan Instrument Company (Yangzhou, China). The maximum test force of the testing machine was 300 kN, which could meet the rigidity requirement of the fracture test. The effective width of the test operation was 445 mm, and the maximum

height of the test was 950 mm. The loading method was constant displacement, and the loading rate was 0.15 mm/min. It took about 40–60 min for each specimen to be loaded from the beginning to failure. A relatively complete load-crack mouth opening displacement curve was obtained, leading to a continuous and stable wedge-splitting fracture test. The acquisition system of the test data contained a load sensor, a clamp-type extensor for measuring crack opening displacement, a strain gauge for determining crack initiation load, and a multi-channel acquisition box for collecting all data. The load sensor was produced by a Sensor Limited Company called Yuyao Sayers in Zhejiang Ningbo. The type of specification was CS-23, the sensitivity was 1.8 mV/V, the measuring range was 0–30 kN, and the allowed overload was 130%FS. The clip-type extensor in the YYJ-4/10 type was produced by Central Iron and Steel Research Institute in Beijing. The standard distance was 10 mm, the measuring range was 0–4 mm, the measurement accuracy was greater than 0.5%, and the sensitivity was 1.74 mV/V. The testing machine of the wedge-splitting double-K fracture in TY-8000, as well as the test loading process, are shown in Figure 1.



**Figure 1.** TY-8000 testing machine and test loading process diagram.

## 2.2. Experimental Design and Methods

According to the RILEM Standard testing methods for the determination of unstable cracking or failure for predicting crack the double-K criterion for crack propagation in concrete using wedge-splitting tests and three-point bending beam tests, the size of the wedge-splitting fracture test specimen was 330 mm × 300 mm × 120 mm, the size of the reserved groove was 50 mm × 30 mm × 120 mm, and the initial fracture-to-height ratio was 0.4. The mold was a steel mold designed by a self-team, which provided better strength and stiffness. The size of the finished specimens was within the specified error range.

The control factors of the experiment were concrete strength grade and moisture content, and the moisture content was used as the measuring unit of concrete humidity. The strength grades were set as C20, C30, and C40 according to the preset test factors, and the moisture content was set as completely dry to near saturation and five kinds of moisture content in three intermediate humidity states. There were 15 experimental groups with 5 specimens in each group, totaling 75 specimens. Groups A<sub>0</sub>, B<sub>0</sub>, and C<sub>0</sub> were the standard comparison groups under the dry condition, and A<sub>1</sub>–A<sub>4</sub>, B<sub>1</sub>–B<sub>4</sub>, and C<sub>1</sub>–C<sub>4</sub> were tested groups, using different moisture content of C20, C30, and C40 concrete, respectively. The specific experimental groups are set in Table 2. The preparation process of concrete specimens is shown in Figure 2.

**Table 2.** Experimental grouping.

Strength Grade	Completely Dry Group	Soak Time (h)			
		2	5	24	120
C20	A <sub>0</sub>	A <sub>1</sub>	A <sub>2</sub>	A <sub>3</sub>	A <sub>4</sub>
C30	B <sub>0</sub>	B <sub>1</sub>	B <sub>2</sub>	B <sub>3</sub>	B <sub>4</sub>
C40	C <sub>0</sub>	C <sub>1</sub>	C <sub>2</sub>	C <sub>3</sub>	C <sub>4</sub>

**Figure 2.** Concrete specimens were prepared.

The concrete specimens were put into the electro-thermostatic blast oven, and the dried concrete specimens were obtained by 105 °C continuous drying for 120 h, based on the optimal drying process established by the research team. The weight of the dried specimens was  $m_0$  after natural cooling. The moisture content was indirectly controlled by soaking for a different amount of time, and the soaking time of concrete was set as 0 h, 2 h, 5 h, 24 h, and 120 h in a free water environment. The dry specimens were immersed in water to make the water surface rise 2–3 cm beyond the top surface of the specimens, which effectively ensured that the specimens could be completely submerged after absorbing water. The specimens of each group were removed after reaching the preset soaking time, then the surface was wiped with a damp cloth so that the surface remained moist without water droplets. The mass of the specimens removed after the soaking time  $T$  was  $m_T$ . In order to prevent mass loss due to collision during the weighing and unloading of the specimen, the specimen should be handled gently throughout the whole process. By intermittently recording the mass change process of 15 test group specimens after different soaking times, the moisture content of concrete was calculated according to Formula (1). The moisture content of the wedge-splitting specimens in each test group was the average value of 5 specimens. The soaking process of concrete specimens is shown in Figure 3. The mechanical properties of double-K fractures of concrete specimens after different soaking times were measured, and the change rule of mechanical properties of concrete with different moisture contents was obtained.

$$\rho_T = \frac{m_T - m_0}{m_0} \times 100\% \quad (1)$$

where:  $\rho_T$  is the moisture content of concrete specimen with  $T$  soaking time, %.  $m_T$  is the mass of concrete specimen with  $T$  immersion time, kg.  $m_0$  is the mass of dry concrete specimen, kg.



**Figure 3.** The concrete specimens were soaked in a watery environment.

### 3. Result and Discussion

#### 3.1. Variation Rule of Concrete Moisture Content

According to the mass changes of 15 test specimens after different soaking times, the moisture content of each specimen was calculated according to Formula (1), and the water absorption quality data of 75 wedge-split concrete specimens were obtained in total. In order to ensure the rationality of the test data, moisture content exceeding 15% of the average value was eliminated, then the average value of the remaining moisture content was calculated as the final average moisture content. The results of the calculation of moisture content of concrete specimens with different strength grades after soaking for different times are shown in Table 3.

**Table 3.** Relationship between moisture content and soaking time.

Strength Grade	Moisture Content (%)				
	0	2 h	5 h	24 h	120 h
C20	0	4.282	5.272	5.570	5.811
C30	0	3.603	4.850	5.599	5.662
C40	0	3.246	4.690	5.347	5.456

Water absorption by concrete soaking was a slow and complex process, which could not reach the absolute saturation in a short time. Therefore, the saturated moisture content in this study was defined as the moisture content when the mass increase of the specimen was less than 2 g/h per unit of time during the soaking process, which was the approximate saturation. As shown in Table 3, with the increase of soaking time, the moisture content of concrete specimens rapidly increased in the early stage and increased slowly until constant in the late stage; the C40 concrete specimen absorbed water rapidly, and the moisture content increased rapidly. The moisture content was about 85% of the saturated state after soaking for 5 h. The moisture content of the specimens increased slowly for 5–24 h and reached 95% of the saturated state after soaking for 24 h. The concrete of each strength grade had reached the approximate saturation after soaking for 120 h.

When the soaking time was the same, the concrete strength grade was higher, the water absorption rate was slower, and the moisture content was lower. For example, when the soaking time was 5 h, the moisture content of C20, C30, and C40 concrete was 5.272%, 4.850%, and 4.690%, respectively, and the moisture content of C20 concrete was 1.12 times that of C40. When the concrete specimen reached the saturation state, the grade of concrete specimen strength was higher, the saturated moisture content was lower, and the water

absorption time was longer. For example, the saturated moisture content of C40 concrete was 93.8% of that of C20 concrete. The concrete strength grade was higher, the concrete as a whole was denser, and the internal porosity was lower; thus, the moisture content of concrete was affected by the strength grade.

### 3.2. Variation Rule of Fracture Toughness of Wet Concrete

#### 3.2.1. Determination of Fracture Parameters of Double-K under Different Moisture Content

According to the RILEM Standard Testing methods for determination of unstable cracking or failure for predicting crack the double-K criterion for crack propagation in concrete using wedge-splitting tests and three-point bending beam tests [31], crack initiation load was a nonlinear turning point on the load–crack mouth opening displacement curve. In the process of measurement, it was difficult to determine the crack initiation load directly on the whole curve, so it needed to be measured indirectly using other methods. In this paper, the simple and intuitive resistance strain gauge method was used, which involved a pair of resistance strain gauges arranged 10 mm apart from the prefabricated crack tip to observe the initiation load, and the curve of load strain with the crack tip was obtained.

Experimental studies showed that it was accurate and feasible to use the resistance strain gauge method to measure concrete initiation load, and the formula for calculating cracking fracture toughness is shown in (2)–(4).

$$P_{HQ} = \frac{P_Q + mg \times 10^{-2}}{2 \tan 15^\circ} \quad (2)$$

$$K_{IC}^{ini} = \frac{P_{HQ} \times 10^{-3}}{tW^{\frac{1}{2}}} f(\alpha) \quad (3)$$

$$f(\alpha) = \frac{3.675[1 - 0.12(\alpha - 0.45)]}{(1 - \alpha)^{3/2}}, \quad \alpha = \frac{a_0}{W} \quad (4)$$

where:  $P_Q$  is vertical initiation load, kN.  $m$  is mass of wedge loading frame, kg.  $g$  is acceleration of gravity and is  $9.81 \text{ m/s}^2$ .  $P_{HQ}$  is horizontal initiation load, kN.  $K_{IC}^{ini}$  is initiation fracture toughness,  $\text{MPa}\cdot\text{m}^{1/2}$ .  $t$  is thickness of specimen, mm.  $W$  is effective height of specimen, mm.  $a_0$  is initial fracture length, mm.  $\alpha$  is initial peak ratio, dimensionless.

The peak load and critical crack opening displacement were measured throughout the test, then the elastic model E was calculated, and lastly the unstable fracture toughness was calculated. The specific calculation formulas are shown in (5)–(10):

$$P_{Hmax} = \frac{P_{Vmax} + mg \times 10^{-2}}{2 \tan 15^\circ} \quad (5)$$

$$K_{IC}^{un} = \frac{P_{Hmax} \times 10^{-3}}{tW^{\frac{1}{2}}} f(\alpha) \quad (6)$$

$$f(\alpha) = \frac{3.675[1 - 0.12(\alpha - 0.45)]}{(1 - \alpha)^{3/2}}, \quad \alpha = \frac{a_c}{W} \quad (7)$$

$$a_c = (W + h_0) \left[ 1 - \left\{ \frac{13.18}{\frac{CMOD_C \times E \times t}{P_{Hmax}} + 9.16} \right\}^{\frac{1}{2}} \right] - h_0 \quad (8)$$

$$E = \frac{1}{tc_i} \left[ 13.18 \left( 1 - \frac{a_0 + h_0}{h + h_0} \right)^{-2} - 9.16 \right] \quad (9)$$

$$c_i = \frac{CMOD_{ci}}{P_i} \quad (10)$$

where:  $P_{Vmax}$  is vertical peak load, kN.  $P_{Hmax}$  is horizontal peak load, kN.  $K_{IC}^{un}$  is unstable fracture toughness,  $\text{MPa}\cdot\text{m}^{1/2}$ .  $a_c$  is effective fracture length, mm.  $\sqrt{h_0}$  is thickness of stainless-steel sheet used for clamping extension meter knife edge, mm.  $CMOD_C$  is critical fracture opening displacement, mm.  $E$  is calculation of elastic modulus, GPa.  $h$  is specimen

height, mm.  $c_i$  is initial  $CMOD_C/P$  value of specimen,  $\mu\text{m}/\text{kN}$ , calculating by  $F_i$ ,  $CMOD_{c_i}$  at any point in the line segment of the ascending section of the  $P - CMOD_C$  curve of the specimen.

The fracture energy of the concrete was the average energy consumed by crack propagation per unit area, which took into account the ratio of the work done to the specimen using external loads, including the dead weight of the loading frame, to the area of the crack ligament (the area of the crack propagation area projected on the plane parallel to the direction of the main crack). Characterizing the ability of concrete material to resist crack propagation was an important parameter which could not be ignored in the study of concrete fracture properties. The concrete fracture energy is calculated according to Formula (11) [37].

$$G_F = \frac{Q}{A_{lig}} = \frac{\int_0^{CMOD_0} P_{Hd} CMOD + mg \times CMOD_0}{t(W - a_0)} \quad (11)$$

where:  $G_F$  is fracture energy of concrete,  $\text{N}/\text{m}$ .  $Q$  is work of fracture,  $\text{J}$ .  $A_{lig}$  is area of fracture ligament,  $\text{mm}^2$ .  $CMOD_0$  is maximum opening displacement of crack mouth,  $\text{mm}$ .

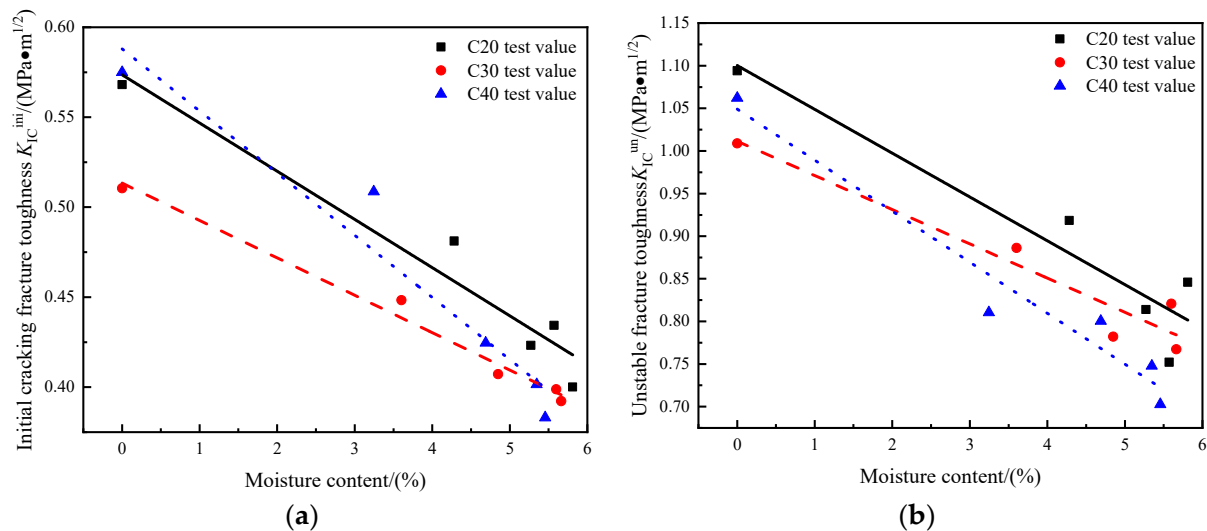
Note: The provenience of Equations (2) through (10) are quoted from RILEM Standard testing methods for determination of unstable cracking or failure for predicting crack the double-K criterion for crack propagation in concrete using wedge-splitting tests and three-point bending beam tests.

### 3.2.2. Influence of Moisture Content on Double-K Fracture Toughness of Concrete

$CMOD_C$ ,  $P_{Vmax}$ ,  $P_Q$ , and other parameters obtained from wedge-splitting tests were put into Formulas (2)–(10) to calculate the initiation fracture toughness and unstable fracture toughness of concrete,  $K_{IC}^{ini}$  and  $K_{IC}^{un}$  under different moisture content are summarized in Table 4. The test values of initiation fracture toughness and unstable fracture toughness of concrete with different strength grades under different moisture content are shown in Figure 4a,b. As shown in Figure 4, the initiation fracture toughness ( $K_{IC}^{ini}$ ) and unstable fracture toughness ( $K_{IC}^{un}$ ) of concrete with different strength grades were significantly affected by moisture content, but the variation rule had a certain dispersion. In the process of C20, C30, and C40 concrete from drying to saturation, the initiation fracture toughness and unstable fracture toughness showed a linear, decreasing trend with the increase of moisture content. Using the experimental group ( $A_4$ ,  $B_4$ , and  $C_4$ ) soaking for 120 h as an example, the moisture content of the group was 5.811%, 5.662%, and 5.456%, respectively. Compared with the drying group ( $A_0$ ,  $B_0$ , and  $C_0$ ) with a moisture content of zero, the initiation fracture toughness ( $K_{IC}^{ini}$ ) of the experimental group ( $A_4$ ,  $B_4$ , and  $C_4$ ) was only 70.4%, 76.8%, and 66.6% of that of drying group ( $A_0$ ,  $B_0$ , and  $C_0$ ), with a decrease of 29.6%, 23.2%, and 33.4%, respectively. Similarly, using the experimental group ( $A_4$ ,  $B_4$ , and  $C_4$ ) soaking for 120 h as an example, the unstable fracture toughness ( $K_{IC}^{un}$ ) of the group was 77.3%, 76.1%, and 66.2% of that of the drying group ( $A_0$ ,  $B_0$ , and  $C_0$ ), with a decrease of 22.7%, 23.9%, and 33.8%, respectively. When water with a pressure of 0.3 MPa was present in a precast crack of concrete, studies in the literature [23,38] showed that the cracking initiation toughness of saturated concrete is 34.0% and 21.8% lower than that of dry concrete. When the three-point bending beam fracture test method was adopted, the conclusion of the literature [30] was that the cracking initiation toughness of saturated concrete was reduced by 41.9%, compared with that of completely dry concrete. The definitions of the dry and saturated state of concrete in this paper were different from the above researchers, as well as the strength mix ratio of concrete samples, fracture mechanical properties test methods and other test conditions; thus, the decline range was different, but the change trend was consistent.

**Table 4.** Fracture parameters of concrete specimens with different moisture content.

Test Grouping	$CMOD_C$ (%)	$P_{HQ}$ (kN)	$P_{Hmax}$ (kN)	$a_c$ (mm)	$K_{IC}^{ini}$ (Mpa·m <sup>1/2</sup> )	$K_{IC}^{un}$ (Mpa·m <sup>1/2</sup> )
A <sub>0</sub>	0.231	4.70	6.49	155.60	0.57	1.09
A <sub>1</sub>	0.174	4.14	5.24	165.06	0.48	0.92
A <sub>2</sub>	0.151	3.50	4.91	154.79	0.42	0.81
A <sub>3</sub>	0.148	3.59	4.59	154.15	0.43	0.75
A <sub>4</sub>	0.148	3.31	4.59	173.24	0.40	0.85
B <sub>0</sub>	0.194	4.22	6.04	156.33	0.51	1.01
B <sub>1</sub>	0.182	3.71	5.18	158.96	0.45	0.89
B <sub>2</sub>	0.163	3.36	4.80	153.72	0.41	0.78
B <sub>3</sub>	0.155	3.30	4.76	159.64	0.40	0.82
B <sub>4</sub>	0.156	3.24	4.44	159.39	0.39	0.77
C <sub>0</sub>	0.173	4.75	6.50	153.26	0.57	1.06
C <sub>1</sub>	0.163	4.20	5.33	146.44	0.51	0.81
C <sub>2</sub>	0.157	3.51	4.91	153.76	0.42	0.80
C <sub>3</sub>	0.142	3.32	4.63	152.83	0.40	0.75
C <sub>4</sub>	0.134	3.17	4.27	152.83	0.38	0.70

**Figure 4.** Experimental values of initial cracking fracture toughness and unstable fracture toughness of concrete under different moisture content. (a) Initial cracking fracture toughness (b) Unstable cracking fracture toughness.

The deterioration degree of the double-K fracture toughness of concrete under moisture content condition must be studied. The absolute difference between crack initiation fracture toughness ( $K_{IC}^{ini}$ ) and unstable fracture toughness ( $K_{IC}^{un}$ ) of concrete under different moisture contents and dry conditions was defined as the deterioration value of crack initiation toughness ( $\Delta K_{IC}^{ini}$ ) and unstable toughness deterioration value ( $\Delta K_{IC}^{un}$ ). The degradation values of crack initiation toughness and unstable toughness of concrete with different strength grades under different moisture content states are shown in Figure 5a,b. As shown in Figure 5, the degradation values of crack initiation toughness and unstable toughness of concrete with C20, C30, and C40 under different moisture content states were essentially similar. The deterioration value of crack initiation toughness and unstable toughness showed a linear, increasing trend with the increase of moisture content. For concrete with the same strength grade where the moisture content was higher, the deterioration value of crack initiation toughness and unstable toughness would be higher. For example, when the moisture content was 2%, the cracking toughness deterioration values of C20, C30, and C40 concrete were 0.049 Mpa·m<sup>1/2</sup>, 0.039 Mpa·m<sup>1/2</sup>, and 0.057 Mpa·m<sup>1/2</sup>, respectively. When the moisture content of C20, C30, and C40 concrete was 5%, the degradation val-

ues of cracking toughness were  $0.130 \text{ Mpa}\cdot\text{m}^{1/2}$ ,  $0.102 \text{ Mpa}\cdot\text{m}^{1/2}$ , and  $0.162 \text{ Mpa}\cdot\text{m}^{1/2}$ , respectively, which were 2.65, 2.62, and 2.84 times greater than the moisture content in 2%. When the moisture content was 5%, the deterioration values of unstable toughness of C20, C30, and C40 concrete were  $0.249 \text{ Mpa}\cdot\text{m}^{1/2}$ ,  $0.197 \text{ Mpa}\cdot\text{m}^{1/2}$ , and  $0.313 \text{ Mpa}\cdot\text{m}^{1/2}$ , respectively, which were 2.59, 2.56, and 2.35 times greater than the moisture content in 2%, which was 2.5 times closer to the increase of moisture content. When the moisture content of the concrete was the same, the degradation value of crack initiation toughness and unstable toughness of C40 concrete was the largest, followed by C20 concrete, and then C30 concrete.

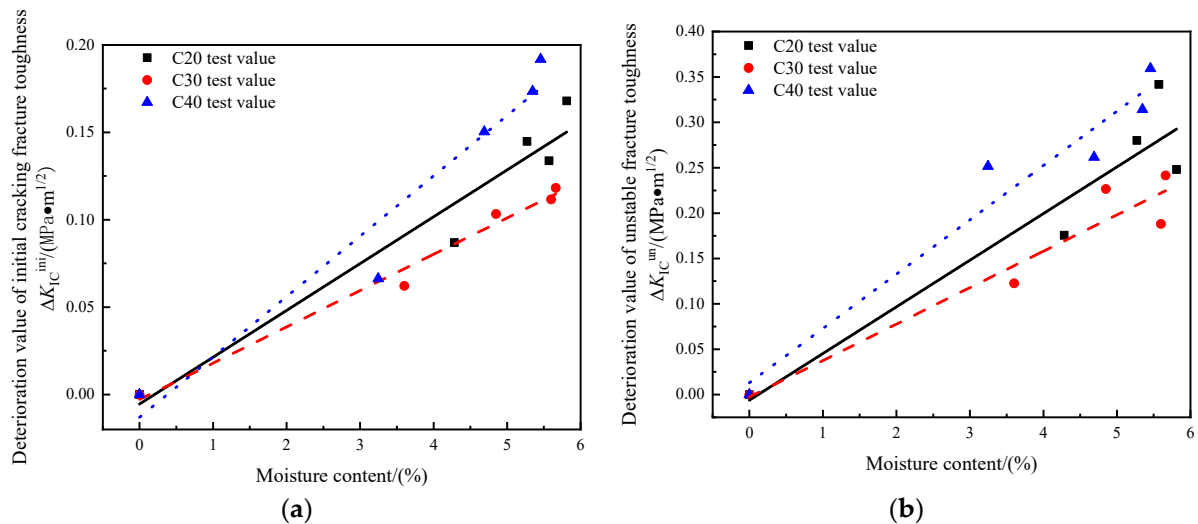


**Figure 5.** Variation curve of deterioration value of initial cracking fracture toughness and unstable fracture toughness of concrete under different moisture content. (a) Deterioration value of initial cracking fracture toughness (b) Deterioration value of unstable fracture toughness.

### 3.3. Fracture Failure Deformation Characteristics at Different Moisture Contents

The horizontal load–crack opening displacement curves of C20, C30, and C40 concrete under different moisture content conditions are shown in Figure 6a–c. According to Figure 6, the variation rule of  $P_H$ – $CMOD$  curves of C20, C30, and C40 concrete under different moisture content was essentially the same, and the critical crack mouth opening displacement gradually decreased with the increase of moisture content. For example, C20 concrete  $CMOD_C$  in the dry state was 1.56 times greater than in the saturated state. The fracture deformation under different moisture content can be divided into three stages.

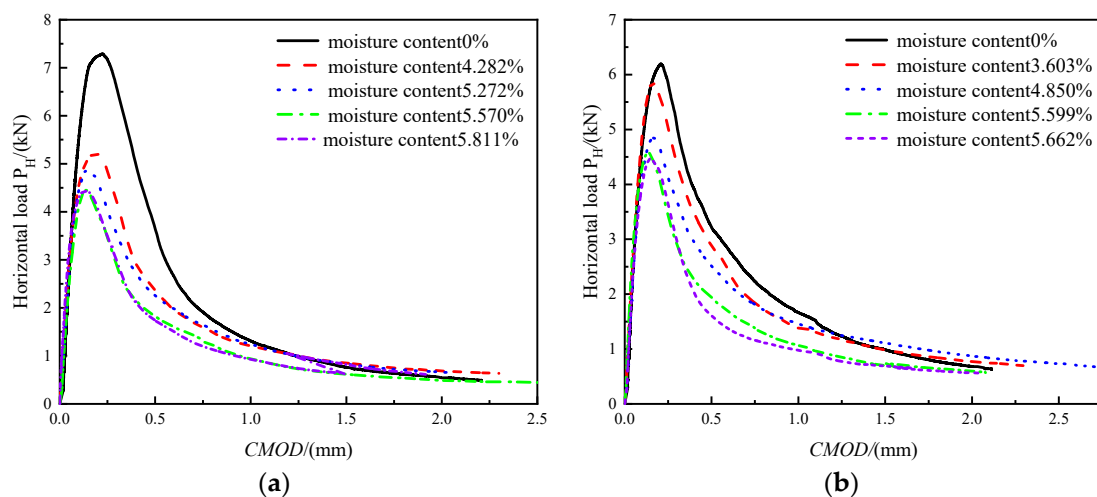


**Figure 6.** Cont.

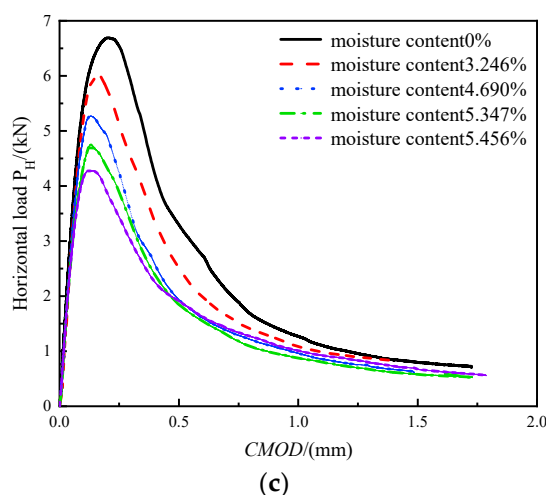


**Figure 6.** Typical  $P_H$ – $CMOD$  curve of concrete with different moisture content and strength grade. (a)  $P_H$ – $CMOD$  curve of C20 concrete (b)  $P_H$ – $CMOD$  curve of C30 concrete (c) Typical  $P_H$ – $CMOD$  curve of C40 concrete.

1. Linear elastic non-crack initiation stage ( $K < K_{IC}^{ini}$ ). At the beginning of the loading stage, elastic deformation occurred in the concrete, and no-cracking initiation occurred in the ligament area at the precast crack tip, and the crack mouth opening displacement  $CMOD$  showed a rapid and linearly increasing trend with the increase of the load. At this time, the  $P_H$ – $CMOD$  curve was straight, and the crack initiation load was about 60–80% of the maximum load. The linear elastic section of completely dry concrete was the longest. The slope of the ascending section and the length of the linear section showed a gradually decreasing trend with the increase of moisture content.

2. Stable expansion stage ( $K_{IC}^{ini} < K < K_{IC}^{un}$ ). Microcracks appeared in the ligament area with a further increase of the load. At this time, the  $P_H$ – $CMOD$  curve turned into a nonlinear stage, and the slope gradually decreased until the horizontal load neared the peak value. Moisture had an enhanced effect on the stable expansion stage of concrete, which was when the slope of  $P_H$ – $CMOD$  curve showed a decrease alongside the increase of moisture content in the stable expansion stage. The stable expansion stage of dry concrete was the longest, and it became shorter with the increase of moisture content.

3. Unstable expansion stage ( $K > K_{IC}^{un}$ ). It began to unload when the peak load was reached, then the prefabricated crack began to expand rapidly, which is when the slope of the  $P_H$ – $CMOD$  curve showed a rapid, negative growth and the crack opening displacement increased slowly. When the load was unloaded to 1/3 of the peak load, the slope change showed an inflection point, and the slope then gradually decreased until it was close to zero. When the  $CMOD$  was the same, the moisture content was greater, the corresponding horizontal load was lower, and the decline of the  $P_H$ – $CMOD$  curve was gentler in the unstable expansion stage. For example, the horizontal load of dried concrete was 6.69 kN when the  $CMOD$  of C40 concrete was 0.2 mm, while the horizontal load of saturated concrete was 3.874 kN, which is 42.1% lower than that of dried concrete.

The crack mouth opening displacement of  $CMOD_C$ , corresponding to the peak load of C20, C30, and C40 concrete under different moisture content conditions, was summarized to obtain the change curve of concrete critical crack opening displacement under different moisture content conditions (Figure 7). As shown in Figure 5, the  $CMOD_C$  of concrete specimens in wedge-splitting decreased with an increase in moisture content. For example, the  $CMOD_C$  of C20, C30, and C40 concrete under saturated condition decreased by 35.93%, 19.41%, and 22.45%, respectively, compared with that under the dry condition. Under the same moisture content of concrete, the concrete strength grade was higher, the  $CMOD_C$  was smaller. For example, the  $CMOD_C$  of C40 concrete was 84.06% and 91.09% of that of C20 and C30 concrete, respectively, when the moisture content was 2% for both. The concrete

low-strength grade  $CMOD_C$  dropped more significantly under the same moisture content. Compared with the C20 concrete in the dry state, the reduction of C20 concrete  $CMOD_C$  in saturation was 1.85 times and 1.6 times of C20 and C30 concrete, respectively, indicating that concrete low-strength grade  $CMOD_C$  was more sensitive to moisture content. Concrete in the dry condition had good toughness. With moisture in the concrete interior, the deformation and toughness of concrete became worse. On the macro level, the critical crack opening displacement gradually decreased, which led to the deterioration of concrete cracking resistance.

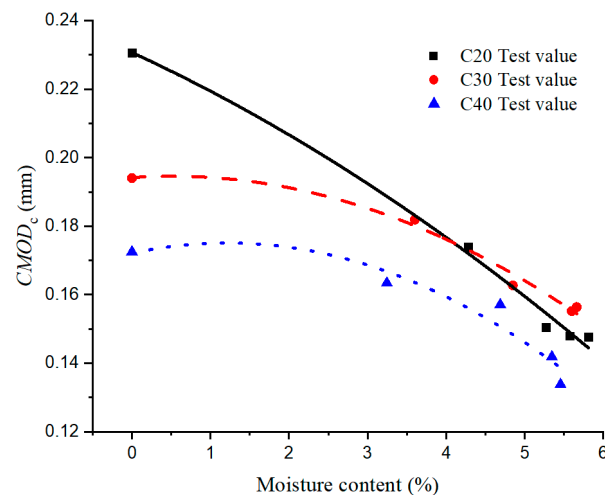


**Figure 7.** The critical fracture opening displacement  $CMOD_C$  varies with moisture content.

### 3.4. Influence Rule of Moisture Content on Concrete Fracture Energy

According to the experimental test results, the concrete fracture energy under different moisture content conditions can be calculated according to Formula (11). Figure 8 shows the concrete fracture energy curve with different moisture contents. As shown in Figure 8, the fracture energy ( $G_F$ ) of C20, C30, and C40 concrete showed a nonlinear, decreasing trend with the increase of moisture content, and the influence of moisture content was significant. The C20, C30, and C40 concrete fracture energy in the saturated state was only 71.99%, 70.29% and 66.11% of that in dry state. Under the same moisture content condition, the concrete strength grades were higher and the fracture energy reduction was greater. For example, when the concrete functional rates were all 4.29%, the C20, C30, and C40 concrete fracture energy was reduced by 7.96%, 6.23%, and 1.58%, respectively, compared to the dry state.

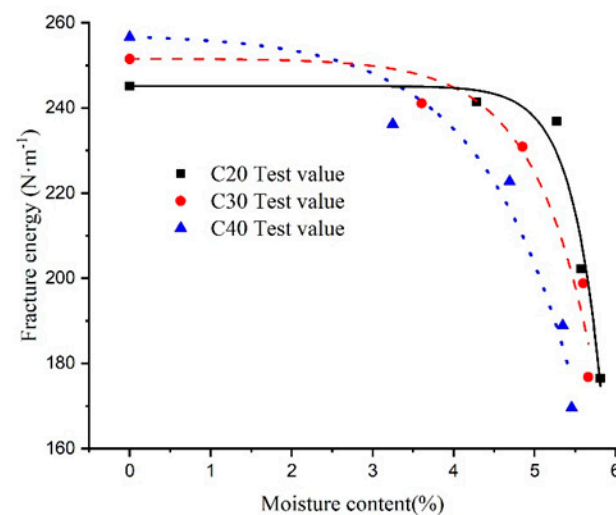


**Figure 8.** Fracture energy curve of concrete with different moisture content.

It was worth noting that the variation amplitude of concrete fracture energy in different moisture content ranges differed significantly with the increase of moisture content. The changing process of concrete fracture energy with moisture content from the dry to the saturated state could be roughly divided into three stages: slow descent, transitional descent, and rapid descent stage. Using C30 concrete as an example, the specific change rule of each stage was as follows: (1) Slow descent stage ( $\rho < 3.6\%$ ). In the early stage of concrete-free water absorption, when the concrete moisture content gradually increased to 3.6%, the concrete fracture energy slowly decreased alongside an increase in moisture content. The fracture energy decreased by 4.11%, compared with the dry state when the moisture content increased by 3.6 times. (2) Transitional descent stage ( $3.6\% < \rho < 4.9\%$ ). The reduction rate of concrete fracture energy gradually increased alongside a continuous increase in moisture content. At this stage, the moisture content was increased by 1.36 times, and the corresponding fracture energy was decreased by 4.20%. (3) Rapid descent stage ( $\rho > 4.9\%$ ). The concrete fracture energy decreased rapidly when the concrete moisture content was close to saturation. The moisture content was increased from 4.9% to 5.66%, then the moisture content was increased by 1.17 times, and the corresponding fracture energy was decreased by 23.43%.

#### 4. Conclusions

Based on physical tests, this paper obtained the macroscopic law of concrete fracture mechanical properties changing with moisture content but did not carry out further research on the causes of microcosmic changes, which need to be discussed and improved in the future research work. The specific conclusion was as follows:

1. Concrete low-strength grades were more sensitive to moisture content. They quickly absorbed water in the short term, and the water absorption rate was rapidly increased. After soaking for 120 h, each concrete strength grade could reach an approximate saturation, and the approximate saturated moisture content of C20, C30, and C40 concrete was 5.811%, 5.662%, and 5.456%, respectively.
2. The crack initiation fracture toughness and unstable fracture toughness of concrete decreased with the increase of moisture content. The crack initiation fracture toughness of C20, C30, and C40 concrete under saturated state was decreased by 29.6%, 23.2%, and 33.4%, respectively, compared with the dry state. The unstable fracture toughness decreased by 22.7%, 23.9%, and 33.8%, respectively, compared with the dry condition. The decrease in amplitude of initiation fracture toughness and unstable fracture toughness of concrete was essentially similar under the same moisture content.
3. The concrete fracture energy showed a nonlinear, decreasing trend with the increase of moisture content, and the variation amplitude of different moisture content ranges was significantly different. Concrete moisture content from the dry to the saturated state, the changing process of concrete fracture energy could be roughly divided into the slow descending stage, transitional descending stage, and fast descending stage. The fracture energy of C20, C30, and C40 concrete in the saturated state was only 71.99%, 70.29%, and 66.11%, respectively, of that in the dry state. Under the same moisture content condition, the concrete strength grade was higher, and the fracture energy reduction was greater.
4. The  $P_H$ - $CMOD$  relation curve of wet concrete could be divided into three stages; namely, linear elasticity, stable crack expansion, and unstable crack expansion. With the increase of moisture content, the slope and length of the linear elastic stage gradually decreased, the slope of the stable expansion stage gradually decreased, and the curve of the unstable expansion stage gently decreased. The critical crack opening displacement gradually decreased alongside an increase in moisture content, the concrete deformation capacity was reduced, and the toughness was gradually reduced.

**Author Contributions:** Data curation, X.N., X.W. and Y.G.; Formal analysis, Z.Y.; Funding acquisition, G.Z.; Investigation, X.N.; Methodology, G.Z., X.N., X.W. and Y.G.; Resources, G.Z.; Software, Z.Y.; Writing—original draft, X.N. and X.W.; Writing—review & editing, G.Z. All authors have read and agreed to the published version of the manuscript.

**Funding:** This research was supported by Yunnan Fundamental Research Projects (2019FD052, 202201AT070104).

**Data Availability Statement:** The data presented in this study are available on request from the corresponding author.

**Acknowledgments:** The authors would like to thank the anonymous reviewers for their constructive suggestions to improve the quality of the paper.

**Conflicts of Interest:** The authors declare no conflict of interest.

## References

1. Bazant, Z.P.; Rajapakse, Y.D.S. *Fracture Scaling*; Springer: Dordrecht, The Netherlands, 2013.
2. Yin, X.; Li, Q.H.; Wang, Q.M.; Reinhardt, H.W.; Xu, S.L. The double-K fracture model: A state-of-the-art review. *Eng. Fract. Mech.* **2023**, *277*, 108988. [[CrossRef](#)]
3. Zang, C.H.; Yang, S.T.; Jin, L.L. Determination of double-K fracture parameters of seawater sea sand concrete. *Ocean Eng.* **2019**, *37*, 142–150.
4. Wang, Q.F.; Liu, Y.H.; Peng, G. Experimental study of dynamic compression properties of concrete subjected to water pressure. *J. Exp. Mech.* **2017**, *32*, 385–396.
5. Dolati, S.S.K.; Armin, M. Review of available systems and materials for splicing prestressed-precast concrete piles. *Structures* **2021**, *30*, 850–865. [[CrossRef](#)]
6. Ryu, D.W.; Ko, J.W.; Kanematsu, M.; Noguchi, T. Study on the moisture distribution in concrete associated with change of environmental conditions. *J. Struct. Constr. Eng.* **2007**, *612*, 5–6.
7. Wang, H.L.; Tian, Y.; Yin, W.W.; Sun, X.Y.; Zou, D.Q. Numerical simulation on the dynamic compressive performances of concretes with different moisture contents. *J. Hydrol. Eng.* **2020**, *51*, 421–429.
8. Tan, C.; Li, Z.L.; Han, J.-S.; Han, J.J.; Du, X.Q. Study on free absorption of concrete with different strength grades and sizes. *Concrete* **2019**, *361*, 34–38.
9. Deng, Y.S.; Wang, H.; Lv, Y.; Wu, P.; Wang, L. Effect of moisture content on the compressive properties of wet concrete. *Concrete* **2017**, *333*, 66–69.
10. Zhang, G.H.; Li, Z.L. Strength of wet concrete under different loading rates. *J. Build. Mater.* **2017**, *20*, 616–622.
11. Salem, S.; Eissa, E.; Zarif, E.; Sherif, S.; Shazly, M. Influence of moisture content on the concrete response under dynamic loading. *Ain Shams Eng. J.* **2022**, *14*, 101976. [[CrossRef](#)]
12. Yuasa, N. Inhomogeneous distribution of the moisture content and porosity from the surface layer to internal parts. *J. Struct. Constr. Eng.* **1998**, *509*, 9–16. [[CrossRef](#)] [[PubMed](#)]
13. Wang, H.L.; Yin, W.W.; Cheng, X.D.; Sheng, Y.F.; Sun, X.Y. Influence of moisture content on dynamic compressive properties of concrete subjected to seismic strain rate. *J. Hydrol. Eng.* **2019**, *50*, 225–232.
14. Han, Y.; Liu, H.B.; Liu, X.P. Study on time-varying law of mechanical properties of wet concrete in the marine environment. *J. Water Harbor* **2020**, *41*, 318–323.
15. Huang, Y.; Xiao, L.; Zhou, Y.; Ding, Y. How First-Immersion Age Affects Wet Expansion of Dam Concrete: An Experimental Study. *Int. J. Civ. Eng.* **2021**, *19*, 441–451. [[CrossRef](#)]
16. Tao, Y.; Lesage, K.; Van Tittelboom, K.; Yuan, Y.; De Schutter, G. Influence of substrate surface roughness and moisture content on tensile adhesion performance of 3D printable concrete. *Cement Concr. Comp.* **2022**, *126*, 104350. [[CrossRef](#)]
17. Zhang, P.; Wei, W.; Shao, Z.; Qiao, R. Effect of moisture on concrete damage and aggregate recycling under microwave irradiation. *J. Build. Eng.* **2022**, *46*, 103741.
18. Zhu, X.; Chen, X.; Bai, Y.; Ning, Y.; Zhang, W. Evaluation of fracture behavior of high-strength hydraulic concrete damaged by freeze-thaw cycle test. *Constr. Build. Mater.* **2022**, *321*, 126346. [[CrossRef](#)]
19. Lu, Y.; Zhu, T.; Li, S.; Liu, Z. Bond behavior of wet-bonded carbon fiber-reinforced polymer-concrete interface subjected to moisture. *Int. J. Polym. Sci.* **2018**, *2018*, 3120545. [[CrossRef](#)]
20. Wang, X.; Petru, M. Experimental study on fracture properties of CFRP-to-concrete interface subject to salt water. *Compos. Struct.* **2021**, *258*, 113179. [[CrossRef](#)]
21. Liu, Z.H.; Hu, Y.; Wu, K.; Yang, N.; Tan, Y.S. Study on fracture development characteristics of low-heat cement concrete at early age. *Yangtze River* **2022**, *53*, 175–181.
22. Xu, H.Y.; Bu, J.W.; Wu, X.Y. Fracture performance and acoustic emission characteristics of dam concrete with different crack-depth ratios. *Water Resour. Power* **2022**, *40*, 100–104.
23. Wang, Y.; Hu, S.W.; Fan, X.Q.; Lu, J. Rate dependence of concrete fracture toughness under water pressure. *Concrete* **2021**, *12*, 20–26.
24. Huang, M.; Zhao, Y.R.; Lin, S.H.; Wang, H.N. Study on fracture damage of BFRPC under freeze-thaw cycles. *Concrete* **2021**, *12*, 31–35.

25. Xu, S.L.; Reinhardt, H.W. Determination of double-determination of double-k criterion for crack propagation in quasi-brittle fracture part i: Experimental investigation of crack propagation. *Int. J. Fract.* **1999**, *98*, 111–149. [[CrossRef](#)]
26. Xu, S.L.; Reinhardt, H.W. Determination of double- k criterion for crack propagation in quasi-brittle fracture, part ii: Analytical evaluating and practical measuring methods for three-point bending notched beams. *Int. J. Fract.* **1999**, *98*, 151–177. [[CrossRef](#)]
27. Xu, S.L.; Reinhardt, H.W. Determination of double-k criterion for crack propagation in quasi-brittle fracture, part iii: Compact tension specimens and wedge splitting specimens. *Int. J. Fract.* **1999**, *98*, 179–193. [[CrossRef](#)]
28. Gao, X.F.; Du, M.; Hu, Y.; Liu, C.F.; Qiao, Y. Experimental study on fracture properties of low heat cement concrete of Baihetan dam. *J. Zhejiang Univ. Technol.* **2021**, *49*, 664–668+698.
29. Xu, S.; Li, Q.; Wu, Y.; Dong, L.; Lyu, Y.; Reinhardt, H.W.; Leung, C.K.Y.; Ruiz, G.; Kumar, S.; Hu, S. Results of round-robin testing for determining the double-K fracture parameters for crack propagation in concrete: Technical report of the RILEM TC265-TDK. *Mater. Struct.* **2021**, *54*, 221. [[CrossRef](#)]
30. Liu, H.J.; Li, Z.L.; Tan, C. Experimental study on influence of different moisture contents on fracture acoustic emission characteristics of concrete. *Adv. Eng. Sci.* **2020**, *52*, 153–161.
31. Zhang, G.H.; Li, Z.L.; Nie, K.Y.; Liu, M.H. Experimental study on fracture toughness of concrete with different moisture contents. *J. Hydraul. Eng.* **2016**, *35*, 109–116.
32. Lou, J.M.; Zhang, G.H.; Yang, Z.D.; Sun, J.C. Experimental study on double K fracture characteristics of wet concrete based on wedge and splitting. *Bull. Chin. Ceram. Soc.* **2022**, *41*, 229–337.
33. He, J.; Shi, J.; Lu, Z. Assessment of interfacial fracture energy between concrete and CFRP under water immersion conditions. *Constr. Build. Mater.* **2021**, *285*, 122942. [[CrossRef](#)]
34. Tian, Y.; Zhao, X.; Zhou, J.; Nie, Y. Investigation on the influence of high-pressure water environment on fracture performance of concrete. *Constr. Build. Mater.* **2022**, *341*, 127907. [[CrossRef](#)]
35. Hu, S.W.; Hu, X.; Fan, B. Effect of defect shape on fracture characteristics of concrete wedge splitting. *Water Resour. Power* **2019**, *37*, 110–113.
36. *DL/T 5330—2015*; Code for Mix Design of Hydraulic Concrete. China Electric Power Press: Beijing, China, 2015.
37. Determination of the fracture energy of mortar and concrete by means of three-point bend tests on notched beams. *Mater. Struct.* **1985**, *18*, 285–290.
38. Wang, Y.; Hu, S.W.; Fan, X.Q.; Lu, J. Effect of water pressure on fracture parameters of concrete. *Constr. Build. Mater.* **2019**, *199*, 613–623. [[CrossRef](#)]

**Disclaimer/Publisher’s Note:** The statements, opinions and data contained in all publications are solely those of the individual author(s) and contributor(s) and not of MDPI and/or the editor(s). MDPI and/or the editor(s) disclaim responsibility for any injury to people or property resulting from any ideas, methods, instructions or products referred to in the content.